

Anisotropic Shape Changes of Silica Nanoparticles Induced in Liquid with Scanning Transmission Electron Microscopy

Jovana Zečević*, Justus Hermannsdörfer, Tobias Schuh, Krijn P. de Jong, and Niels de Jonge*

Jovana Zečević, Krijn P. de Jong

Inorganic Chemistry and Catalysis, Debye Institute of Nanomaterials Science, Utrecht University, 3584 CG Utrecht, The Netherlands

E-mail: J.Zececiv@uu.nl

Justus Hermannsdörfer[†], Tobias Schuh[§], Niels de Jonge

INM–Leibniz Institute for New Materials, Campus D2 2, 66123, Saarbrücken, Germany

Niels de Jonge

Department of Physics, University of Saarland, Campus A5 1, 66123 Saarbrücken, Germany

[†]Present address: Nanoinitiative Bayern GmbH, 97074 Würzburg, Germany

[§]Present address: Enovos Deutschland SE, 66121 Saarbrücken, Germany

E-mail: niels.dejonge@leibniz-inm.de

Liquid-phase transmission electron microscopy (TEM) has been used for in-situ imaging of nanoscale processes taking place in liquid, such as the evolution of nanoparticles during synthesis or structural changes of nanomaterials in liquid environment. Here, we show that the focused electron beam of scanning TEM (STEM) brought about the dissolution of silica nanoparticles in water by a gradual reduction of their sizes, and that silica was re-deposited at the sides of the nanoparticles in the scanning direction of the electron beam, such that

1 elongated nanoparticles were formed. Nanoparticles with an elongation in a different
2 direction were obtained simply by changing the scan direction. Material was expelled from
3 the center of the nanoparticles at higher electron dose, leading to the formation of doughnut-
4 shaped objects. Nanoparticles assembled in an aggregate were found to fuse, and the electron
5 beam exposed section of the aggregate reduced in size and elongated. Under TEM conditions
6 with a stationary electron beam the nanoparticles dissolved but did not elongate. The
7 observed phenomena are important to consider when conducting liquid phase STEM
8 experiments on silica-based materials, and may find future application for controlled
9 anisotropic manipulation of the size and the shape of nanoparticles in liquid.
10
11
12
13
14
15
16
17
18
19
20
21

22 **Keywords:** liquid-phase TEM; liquid-phase STEM; electron beam induced dissolution;
23 anisotropic shape change; electron dose.
24
25
26
27
28
29
30

31 **1. Introduction**

32
33
34 Transmission electron microscopy (TEM) has been a key technique for studying the
35 nanometer-scale morphology of a broad range of samples, for example, catalytic
36 nanoparticleszecevic.^[1-3] However, conventional TEM requires the specimen to be placed in
37 the vacuum of the electron microscope, and thus requires solid samples. With recently
38 developed liquid-phase TEM, samples can be now imaged in a liquid environment.^[4-8]
39
40
41 Liquids are enclosed in specially designed liquid cells usually composed of silicon chips with
42 thin electron transparent silicon nitride windows.^[9-14] It is also possible to image liquid
43 samples in an open vacuum chamber using pump-limiting apertures,^[8] or to study low vapor
44 pressure liquids with standard TEM.^[15] The closed cell type is becoming increasingly popular
45 as it has the potential to provide unique insight into dynamic processes at the nanometer
46 scale, such as nucleation and growth of nanoparticles,^[16-23] dynamic movements of
47
48
49
50
51
52
53
54
55
56
57
58
59
60
61
62
63
64
65

1 nanoparticles,^[11, 12, 24-26] electrochemical deposition and growth of nanoparticles,^[27-30]
2 biomineralization,^[22] and can also be used to study biological function.^[31-33] One of the key
3 challenges liquid-phase TEM faces is to discriminate the phenomena under investigation
4 from electron beam induced effects, such as radiolysis of water in aqueous systems, resulting
5 in the formation of reactive species including e_{aq}^- , H^\bullet , OH^\bullet , H_2 , H_2O_2 , H^+ , OH^- .^[14, 34, 35] The
6 evolution of H_2 through water radiolysis has been linked to the bubble formation within the
7 cell, the creation of e_{aq}^- may trigger the reduction of metal ions in the aqueous solutions,
8 while OH^- and H^+ species can locally change the chemistry of the liquid under
9 examination.^[34] Electron beam induced reduction of metal ions has been the focus of a
10 number of studies in the past years,^[16, 17, 20, 21, 23, 36] while somewhat less attention has been
11 paid to oxide samples.^[37-39] Oxide nanoparticles, such as silica, are important components of
12 materials for biomedical and catalytic applications.^[40-43] Studying their synthesis and
13 behavior under near realistic conditions and at nanoscale in liquid-phase TEM would aid
14 further development of their design. However, like metals, metal-oxides are sensitive to
15 changes in chemical environment, and it is, therefore, crucial to understand which impact
16 radiolysis species and the electron beam can have on silica nanoparticles in liquid-phase
17 TEM.

18 Here, we demonstrate that the combined interaction of radiolysis species and directed
19 electron beam irradiation led to controlled changes in the shape and size of spherical silica
20 nanoparticles. Scanning a focused electron beam over the sample in water appeared to have
21 the power to direct the re-deposition of dissolved silica species on the side of the silica
22 nanospheres thereby causing their elongation. Besides providing background information for
23 future liquid-phase TEM work involving silica, this study presents a phenomenon that can
24 potentially be employed for nanoscale manipulations.

2. Results and Discussion

2.1. Elongation of Nanoparticles

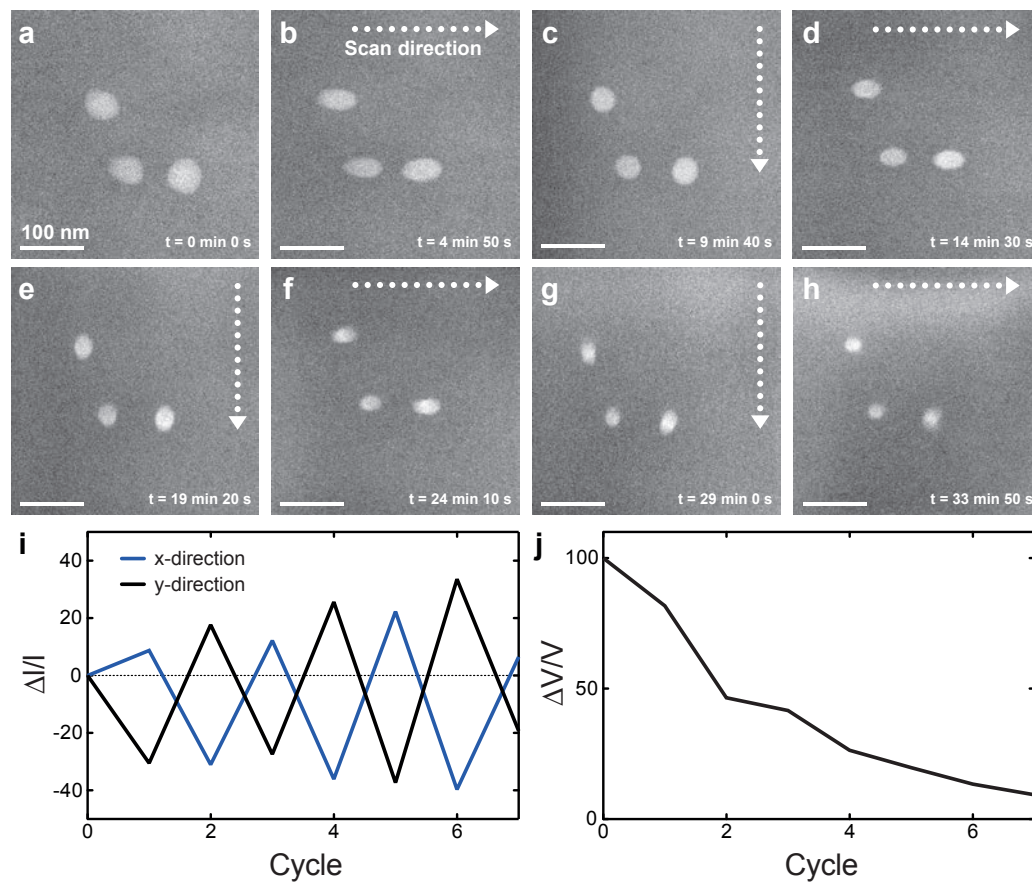


Figure 1. Liquid phase scanning transmission electron microscopy (STEM) images of three silica nanoparticles in pure water acquired at $600,000\times$ magnification (M). The electron dose rate was $3.0 \times 10^3 \text{ e}^-/\text{nm}^2/\text{s}$. (a) Image at the onset of a time-lapse series. (b-h) Images recorded during the exposure to cycles of electron beam scanning with alternating horizontal- and vertical direction. The scan direction is indicated on each figure with the dotted arrow along with the time that lapsed from the beginning of the experiment. Each cycle comprised of 50 STEM images; about 4 min and 50 sec for each cycle, whereby only the last frame of the cycle is shown in the figures b-h. (i) The average change of the sizes ($\Delta l/l$) of the nanoparticles measured in horizontal- and vertical direction per cycle. The electron dose per cycle was $1.0 \times 10^6 \text{ e}^-/\text{nm}^2$. (j) The average calculated volume change ($\Delta V/l$) per cycle.

1 The impact of the water environment and the electron beam on the morphology of the silica
2 nanoparticles was investigated under liquid-phase STEM conditions, and with the water
3 being static in the liquid cell, that is in the absence of liquid flow. Figure 1a shows a STEM
4 image taken at 600,000× magnification (*M*) of three silica nanoparticles spaced at least 30 nm
5 from each other. During nearly 5 min exposure to the focused electron beam with horizontal
6 scanning direction, the elongation of spherical silica nanoparticles in the scan direction was
7 observed, as shown in Figure 1b. The original spherical silica nanoparticles were transformed
8 into ellipsoidal silica nanoparticles.
9

10 To further explore the phenomenon observed in Figure 1b, the scanning direction of
11 the electron beam was rotated by 90°, as indicated in Figure 1c, and the three silica
12 nanoparticles were scanned for another 4 min 50 sec. As can be seen in Figure 1c, the
13 elongated silica nanoparticles from Figure 1b have returned to nearly spherical shape,
14 however, span a smaller area in the image. In total 7 cycles with alternating
15 horizontal/vertical scan direction were performed over nearly 34 min (Supporting Movie 1).
16 In order to remove the water radiolysis species that might cause this silica reshaping and
17 resizing, we performed additional experiments in the flow of water. However, similar effects
18 were observed for the case of a liquid flow through the system (Figure S1), pointing to either
19 insufficient removal of the radiolysis species by water flow or the absence of their impact on
20 the silica reshaping and resizing.
21

22 The directional changes of the nanoparticle shapes were studied from measurements
23 of the widths of the nanoparticles in horizontal- and vertical image direction (see Figure S2
24 and Table S1). It appears that the width of a nanoparticle increased in a direction parallel to
25 the scan direction, while it decreased in perpendicular direction. This directional growth
26 reversed with the rotation of the scan direction by 90 degrees, as shown in Figure 1i. The
27 average increase in any scan direction amounted to 19%, while the decrease amounted to
28
29
30
31
32
33
34
35
36
37
38
39
40
41
42
43
44
45
46
47
48
49
50
51
52
53
54
55
56
57
58
59
60
61
62
63
64
65

1 32% on average. The nanoparticles thus became smaller from cycle to cycle. To estimate the
2 volume, we used the measured horizontal- and vertical widths, and assumed the thickness of
3 a nanoparticle (vertical dimension perpendicular to the image plane) to be equal to the
4 longest of the measured widths. It was indeed verified, by both examining the signal intensity
5 and tilting the particles, that the vertical dimension did not largely reduce or increase (Figures
6 S3 and S4) during the process. The estimated volume change per cycle is shown in Figure 1j.
7 It follows that the volume decreased to ~10% of its original value after 7 cycles. In addition,
8 on the Figures 1g and 1h, light patches indicating the formation of deposit on the Si_xN_y
9 window were observed. To investigate the chemical nature of this deposit we performed
10 energy dispersive X-ray analysis (EDX). It was confirmed that the deposit did not consist of
11 silica that was dissolved from particles, but rather carbon contamination (Figure S5).
12 Furthermore, EDX showed that nanoparticles consisted of silicon oxide.
13
14
15
16
17
18
19
20
21
22
23
24
25
26
27
28

29 **2.2. Model of Anisotropic Shape Change**

30
31 Two distinct phenomena were thus observed, 1) a decrease in volume, and 2) an anisotropic
32 change of shape. Here we propose that the apparent decrease in volume and change of shape
33 of silica nanoparticles is a result of dissolution/re-deposition of silica by the mechanism
34 strongly influenced by the presence of both electron beam and water. The electron caused the
35 exciting of surface silicon (in Figure 2a, Q^2 Si species was used as an example). The excited
36 $\text{Si}^*(\text{OH})_2$ was then more prone to react with water to form silicic acid – $\text{Si}(\text{OH})_4$. Note that
37 under these temperature and pH conditions silica is known to be quite stable in the absence of
38 the electron beam. Part of the formed silicic acid diffused in the liquid, hence causing the loss
39 of silica from the nanoparticles, while another fraction dissociated to form silanolate anions –
40 $\text{Si}(\text{OH})_3\text{O}^-$. From the data we can calculate the amount of irradiating electrons to remove an
41 atom from the silica nanoparticle in water. The most round-appearing nanoparticle shown at
42 the right of Figure 1a has an initial diameter of 53 nm. It was exposed to an electron dose rate
43
44
45
46
47
48
49
50
51
52
53
54
55
56
57
58
59
60
61
62
63
64
65

of $3.0 \times 10^3 \text{ e}^-/\text{nm}^2/\text{s}$, so that the total dose in one cycle of irradiation of 290 sec amounted to $8.6 \times 10^5 \text{ e}^-/\text{nm}^2$. A volume of $9 \times 10^3 \text{ nm}^3$ was removed during this cycle, which translates to 4×10^5 atoms (using a density of 2.2 g/cm^3 and a molar weight of 60 g/mol). Within the initial radiated area, the amount of electrons to remove an atom from the silica nanoparticle in water thus measured 5×10^3 .

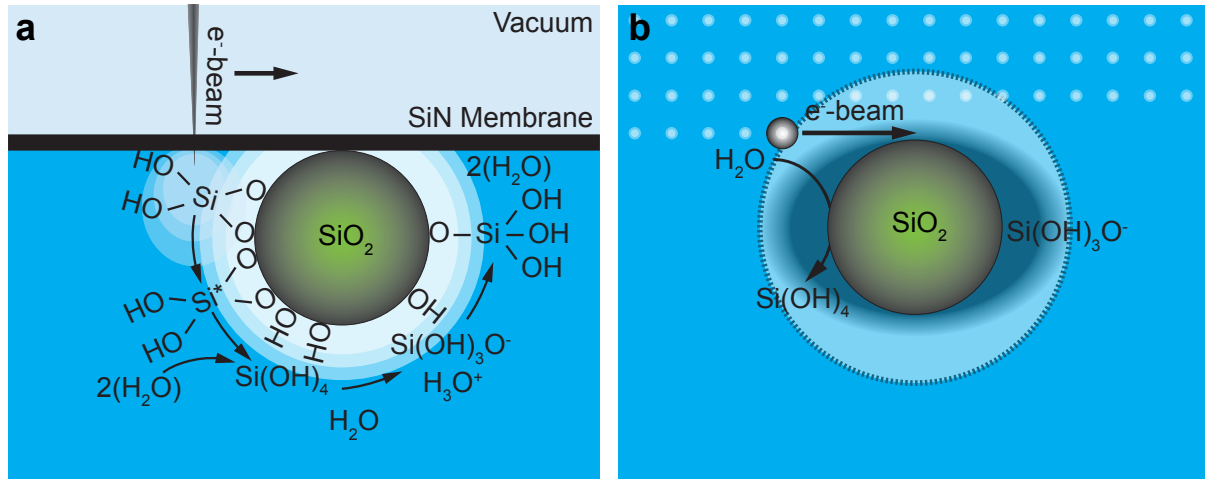


Figure 2. Schematic representation of the proposed mechanism responsible for the elongation of the silica nanoparticles. (a) A focused electron beam scans over a sample in the indicated direction. The sample is water enclosed between silicon nitride membranes containing silica nanoparticles. The electron beam reactions with the surface silicon atoms so that dissolved Si(OH)_4 is formed. Created silicic acid further dissociates to silanolate anion, $\text{Si(OH)}_3\text{O}^-$ of which some deposits on the nanoparticle. (b) Top view of a nanoparticle. As the electron beam scans over the nanoparticle line-by-line an increasing concentration of Si(OH)_4 is created in the middle region (oval shape) at which more nanoparticle surface is irradiated than at the side.

A further effect that probably took place involved the impact of the electron beam with the core of the nanoparticle via inelastic scattering, resulting in ionization and heating of

1 the materials, and also the creation of secondary electrons. These effects tend to destabilize a
2 material. Thirdly, the Si_xN_y membrane probably positively charged on account of secondary
3 electron emission,^[44] which takes place upon irradiation with electron beam, attracting thus
4 part of the dissolved silica species to be deposited at the interface between silica particle and
5 window. Finally, direct removing atoms from the nanoparticle also occurred since the
6 electron beam energy was above knock-on damage threshold for silicon and oxygen. But this
7 effect was apparently not as large as the combined electron beam and water effect causing
8 dissolution/re-deposition of silica, because changes in shape and size of silica nanoparticle
9 were not observed in vacuum for this electron dose (Figure S6).
10
11
12
13
14
15
16
17
18
19
20
21

22 The anisotropic shape change is further explained by the combination of
23 dissolution/re-deposition process of the nanoparticle (Figure 2a) and a concentration effect
24 (Figure 2b). Upon electron beam scanning, the electron probe firstly encountered the side of
25 the nanoparticle (top in Figure 2b). As the electron probe scanned further towards the middle
26 particle, the amount of surface silica species that were excited, dissolved and re-deposited
27 increases, reached a maximum in the middle of the nanoparticle. The areas at those sides of
28 the nanoparticle scanning first and last, respectively, exhibited lower concentrations of
29 dissolved species. This situation is reflected in Figure 2b looking from above the
30 nanoparticle, whereby the concentration gradient of dissolved species is depicted as shaded
31 oval shape.
32
33
34
35
36
37
38
39
40
41
42
43
44
45
46

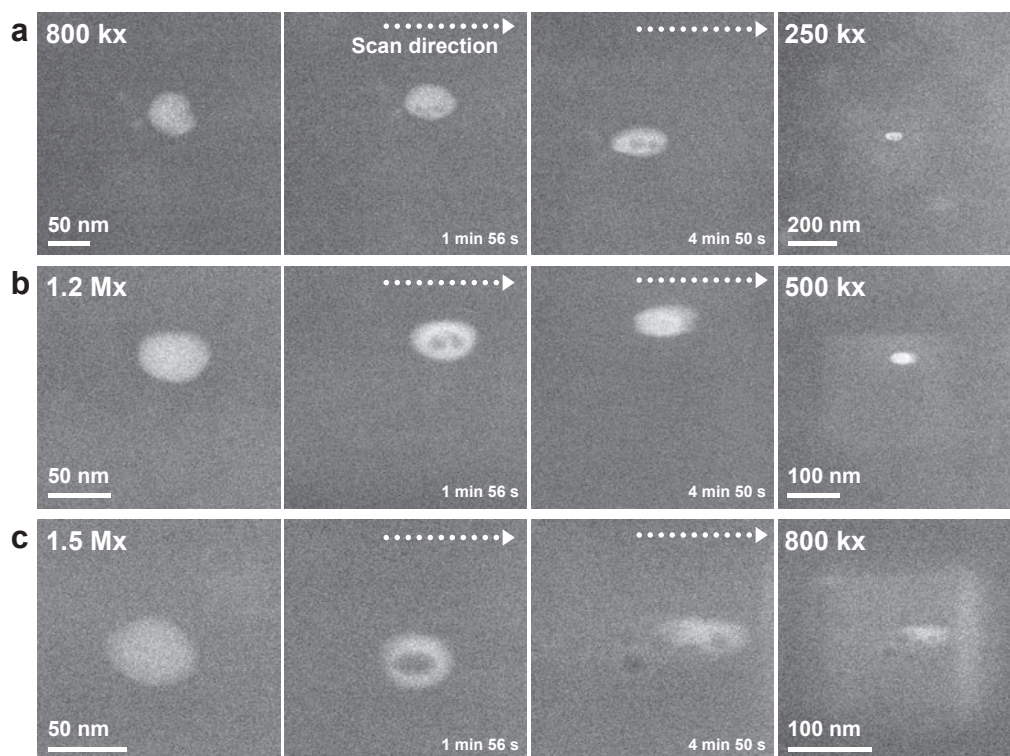
47 It should be noted that the immobilization of the nanoparticles on the supporting
48 Si_xN_y membrane was crucial, while anisotropic concentration gradients would not build if the
49 particles were free to move in the liquid. Yet, freely dispersed silica nanoparticles may
50 become immobilized on the Si_xN_y membrane by the electron beam impact.^[38] The anisotropic
51 effect was not observed for metallic nanoparticles in another study.^[45]
52
53
54
55
56
57
58
59
60
61
62
63
64
65

1 The following other effects are listed for completeness but are unlikely to have happened. It is
2 known that an increase in temperature increases the solubility of silica in water.^[46] However,
3
4 it was calculated by others that a temperature increase in liquid cell is negligible,^[35] which
5
6 rules out the effect of temperature on silica solubility. In theory, mass could have been
7
8 transferred into the axial direction not visible in the two-dimensional projection, thus
9
10 preserving the total volume. However, this does not seem likely because ex-situ images of the
11
12 nanoparticles recorded under a tilt angle did not show enlarged shapes in vertical direction
13
14 (Figure S4). Surface migration and electron beam sputtering may have occurred but would
15
16 not have led to anisotropic shape change and, in particular, reduction in size, but would rather
17
18 have distributed material homogenously over the surface. Plastic deformation of the
19
20 nanoparticle upon irradiation was published for ion-beam irradiation of silica nanoparticles in
21
22 vacuum.^[47] Those authors found an expansion of the nanoparticle in a direction perpendicular
23
24 to the ion beam caused by local heating of the particle. This effect did not likely happen in
25
26 our experiment because in the plane perpendicular to the beam, the nanoparticles showed
27
28 both, expansion and compression. Moreover, the nanoparticles were surrounded by liquid
29
30 with excellent heat conducting properties so that significant temperature changes did not
31
32 likely occur. The observed process is different from experiments in vacuum (Figure S6)
33
34 where some structural rearrangement takes places at very high electron doses but growth in
35
36 one direction and shrinkage in the perpendicular direction is not observed.^[43]
37
38
39
40
41
42
43
44
45

46 **2.3. Creating Holes at Higher Electron Doses**

47
48
49 Upon increasing the magnification, and consequently the total electron dose rate to which the
50
51 nanoparticles were exposed, another interesting phenomenon was observed as well. In Figure
52
53 3, three separate measurements of single silica nanoparticles performed at increasing
54
55 magnifications are shown. The first two measurements were performed with water being
56
57 static in the cell, while the third measurement at $M = 1,500,000\times$ was performed under the
58
59
60
61
62
63
64
65

1 flow of phosphate buffered saline (PBS). During scanning with the electron beam in
 2 horizontal direction, dark oval shapes appeared in all three silica nanoparticles oriented in the
 3 same direction as the nanoparticle elongation. The dark patches indicate a loss of material
 4 from the centers of the nanoparticles because the dark field contrast of STEM results in a
 5 higher signal level at locations with higher (electron) density (Figure S7).
 6
 7
 8
 9
 10
 11



12
 13
 14
 15
 16
 17
 18
 19
 20
 21
 22
 23
 24
 25
 26
 27
 28
 29
 30
 31
 32
 33
 34
 35
 36
 37
 38
 39 **Figure 3.** Liquid-phase STEM time-lapse experiment of individual silica nanoparticles at
 40 increasing magnification. (a) Row of four images of nanoparticles in pure water, $M =$
 41 $800,000\times$. (b) Row of images in pure water recorded at $M = 1,200,000\times$. (c) Images of
 42 nanoparticles in flow of PBS solution, $M = 1,500,000\times$. The leftmost images of the column a-
 43 c show silica nanoparticles before the prolonged exposure to the scanning electron beam.
 44 After 1 min 56 sec of horizontal electron beam scanning (second image column from the
 45 left), dark areas appeared within the nanoparticles indicating a loss of material from their
 46 centers. The higher the magnification was, the larger the loss of material. The nanoparticles
 47 increasingly elongated and reduced their size upon prolonged electron beam scanning, and
 48
 49
 50
 51
 52
 53
 54
 55
 56
 57
 58
 59
 60
 61
 62
 63
 64
 65

1 the effect was the strongest for the highest magnification. Lower magnification images
2 (rightmost column) show a deposition of material in the exposed area.
3
4

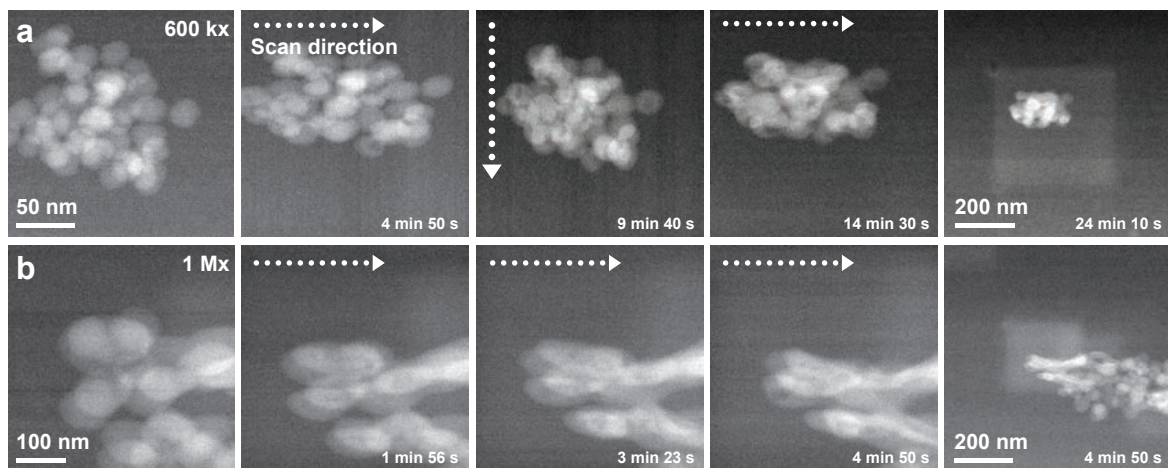
5 The level of structural degradation of the silica nanoparticles became more
6 pronounced with increasing magnification, that is, electron dose rate (Figure 3a-c, second
7 from the left column of images). The holes vanished after 4 min 50 sec of imaging, while the
8 silica nanoparticles became smaller (Figure 3a-c, second from the right column of images).
9
10 At $M = 1,500,000\times$ the nanoparticle was only faintly visible after 4 min 50 sec, indicating a
11 significant loss of material. Low magnification images recorded after 4 min 50 sec scanning
12 (Figure 3a-c, rightmost images), depict lighter patches corresponding to deposits in the areas
13 exposed to the scanning electron beam. This change in contrast was again attributed to
14 deposition of carbon at the vacuum side of the Si_xN_y window (Figure S8).
15
16
17
18
19
20
21
22
23
24
25
26
27

28 Using a salt solution instead of pure water should increase the electrical conductance
29 of the liquid, and possibly reduced the impact of free electrons and charging. However,
30 STEM of silica nanoparticles in PBS at $M = 1,500,000\times$ showed larger shape changes than
31 for pure water at $M = 1,200,000\times$ (Figure 3b and c). Thus, imaging in PBS did not lead to a
32 large reduction of the electron beam effect comparing to the situation in pure water.
33
34
35
36
37
38
39
40
41
42
43
44
45
46
47
48
49
50

51 **2.4. Elongation of Nanoparticles in Aggregates**

52 The behavior of an aggregate of silica nanoparticles under STEM conditions was also
53 investigated. The liquid consisted of either pure water or PBS and was flown through the
54 liquid cell. Comparing Figure 4a left with second from left it can be seen that the silica
55 nanoparticles elongated already after 4 min 50 sec of scanning in horizontal direction. The
56
57
58
59
60
61
62
63
64
65

1 volume reduction was particularly pronounced after the second scan as the nanoparticles
 2 returned to a nearly spherical shape (Figure 4a, middle panel). In addition to the shape and
 3 size changes of the individual silica nanoparticles, it was observed that the entire aggregate
 4 elongated upon horizontal electron beam scanning. After changing the scanning direction to
 5 vertical, and exposing the agglomerate to another 4 min 50 sec of scanning, the aggregate
 6 elongated upon horizontal electron beam scanning. After changing the scanning direction to
 7 vertical, and exposing the agglomerate to another 4 min 50 sec of scanning, the aggregate
 8 returned to its original spherical shape but of a reduced size.
 9
 10
 11
 12
 13
 14



15
 16
 17
 18
 19
 20
 21
 22
 23
 24
 25
 26
 27
 28
 29
 30
 31
Figure 4. Liquid phase STEM of aggregates of silica spheres in a flow of liquid. PBS
 32 solution (a) and in a flow of pure water (b) using STEM. (a) Silica aggregate in a flow of
 33 PBS imaged at $M = 600,000\times$ over a period of about 24 min, with in total of 5 cycles of
 34 alternating scan direction (three shown here). (b) Silica aggregate in pure water was imaged
 35 at $M = 1,000,000\times$ over a period of 4 min 50 sec with the electron beam scanning in the
 36 indicated direction. The rightmost figures show low magnification images completing the
 37 experiment.
 38
 39
 40
 41
 42
 43
 44
 45
 46
 47
 48
 49

50
 51
 52
 53
 54
 55
 56
 57
 58
 59
 60
 61
 62
 63
 64
 65

Possibly, the inter-particle porosity reduced compared to its original structure. It was also found that silica nanoparticles fused, turning the porous silica aggregate (i.e. loosely bound silica particles) into a solid-appearing agglomerate (i.e. particles bound by fusion or sintering) of low porosity as was also observed in a previous study.^[38] After the fifth cycle of scanning had finished (in total about 24 min under electron beam), the size of the silica

1 aggregate was reduced to about half its original size (Figure 4a, rightmost). The same effect
2 of the electron beam on a silica aggregate was observed when water was used instead of PBS
3 (Figure 4b). This experiment revealed an even more pronounced elongation of the individual
4 silica nanoparticles and the aggregate as a whole, ascribed to the higher used magnification
5 and electron dose. Since drastic elongation and fusion of silica nanoparticles already took
6 place after 1 min 56 sec, scanning was only performed in one direction. The directional effect
7 of the scanning electron beam on the shape change of the silica aggregate is best observed at
8 lower magnification (Figure 4b, rightmost). It can be seen that the part of the aggregate that
9 was exposed to the scanning electron beam was completely deformed, while the remaining
10 part of the aggregate still contained spherical silica nanoparticles. Additionally, lighter areas
11 in the scanned region corresponding to deposits of carbon were observed.
12
13
14
15
16
17
18
19
20
21
22
23
24
25
26

27 **2.5. TEM Experiments**

28
29
30 Our results indicate that the focused electron beam of STEM has the capability to reshape
31 silica nanoparticles in aqueous environment. We thus expected that no directional shape
32 change should occur in case of TEM, where the electron beam illuminates the entire field of
33 view instead of being focused, and is not raster-scanned across the sample as in STEM.
34
35 Indeed when silica nanoparticles were imaged using TEM, dissolution of silica and fusion of
36 silica spheres was observed but no elongation or other directional shape changes were seen
37 (Figure 5). Figure 5a shows an aggregate of silica nanoparticles examined under water flow
38 conditions in liquid-phase TEM over a ten-minute period. The shrinkage of the silica
39 aggregates was evident, and accompanied by the fusion of several silica nanoparticles. That
40 silica nanoparticles can completely dissolve under these conditions was confirmed by
41 imaging isolated silica nanoparticles at a higher magnification (Figure 5b). The silica
42 nanoparticle dissolved almost completely after ~10 min. More importantly, in both cases, no
43 elongation of the silica nanoparticles was observed for TEM. It is clear that in case of TEM
44
45
46
47
48
49
50
51
52
53
54
55
56
57
58
59
60
61
62
63
64
65

1
2
3
4
5
6
7
8
9
10
11
12
13
14
15
16
17
18
19
20
21
22
23
24
25
26
27
28
29
30
31
32
33
34
35
36
37
38
39
40
41
42
43
44
45
46
47
48
49
50
51
52
53
54
55
56
57
58
59
60
61
62
63
64
65

imaging where a stationary electron beam is used, the same effect of silica dissolution and fusion takes place, but since there is no directional movement of the beam, as in case of STEM, dissolved silica species are not directionally re-deposited.

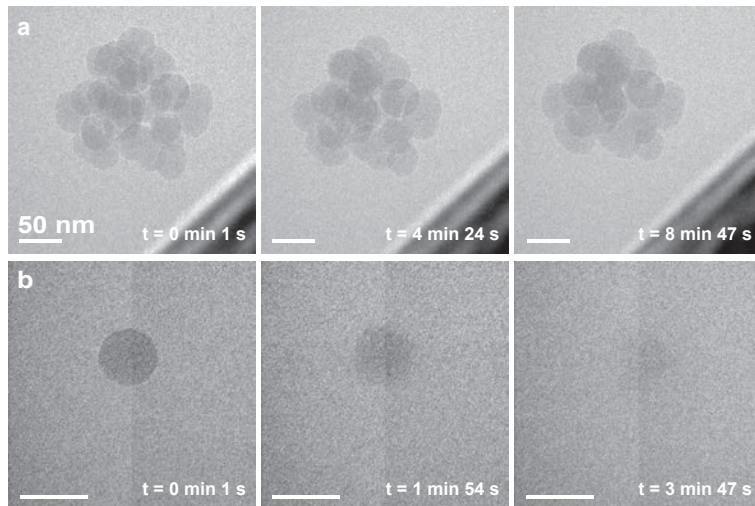


Figure 5. Liquid-phase TEM of silica nanoparticles in a flow of pure water. (a) An aggregate imaged at $M = 250,000\times$. (b) An isolated nanoparticle at $M = 400,000\times$. Each 5 sec a new image was acquired, leading to a total of 100 frames in 9 min 48 sec. Silica dissolved with elapsing time. Scale bars are 50 nm.

3. Conclusions and Outlook

In this work we have demonstrated that the shape and size of silica nanoparticles in a water environment can be manipulated anisotropic by the impact of a focused electron beam. Four distinct effects were observed. Firstly, silica nanoparticles dissolved as was evident from a gradual reduction of their size. Secondly, dissolved silica species were re-deposited on the edges of the silica nanoparticles leading to an elongation of the nanoparticles in the scan direction. Thirdly, more material was removed from the center of the nanoparticles than from their edges at higher electron dose rates, so that doughnut-shaped objects were generated. For the case of silica nanoparticles assembled in aggregates, finally, we observed both the fusing

1 of neighboring nanoparticles and the elongation of the entire section of the aggregate exposed
2 to the electron beam. Notably, the directional re-deposition did not take place under liquid
3 phase TEM conditions. These observations provide new information about the behavior of
4 silica nanoparticles under liquid-phase STEM and TEM conditions. These effects should be
5 considered when designing liquid phase electron microscopy experiments aiming for
6 observing processes happening at the surface of silica nanoparticles. Low dose conditions or
7 a careful selection of the liquid to prevent dissolution of silica would be required to preserve
8 the original structure of the silica nanoparticles, as was shown possible for gold
9 nanoparticles.^[44] As is apparent from the elongation of irradiated nanoparticles in aggregates,
10 it is also possible to modify arrays of silica nanoparticles in parallel. These processes may
11 find future application to the controlled manipulation of the size and the shape of
12 nanomaterials in liquid, whereby materials are created with different properties in different
13 orientations.

34 **4. Experimental Section**

35 *Sample Preparation:* Spherical monodispersed nanoparticles of silica with an average
36 diameter of 50 ± 5 nm were prepared via a procedure adopted from Stöber et al.^[48] A
37 mixture containing 230 ml of ethanol and 11.25 ml of ammonia (Merck, 25%) was stirred,
38 and heated to 35° C. A total of 17.3 g of tetraethyl orthosilicate (TEOS, Aldrich, 98%) was
39 then added, and the solution left to stir for 15 hours at 35 °C. The solution was neutralized
40 with nitric acid (Merck, 65%) and liquid removed using a rotary evaporator. Solid (silica)
41 was dried overnight at 120° C, and calcined in air for 2 h at 200° C, followed by 1 h at 400°
42 C and finally 3h at 600° C. To break the aggregated nanoparticles and thus to expose as much
43 as possible individual silica spheres, the sample was dispersed in ethanol and sonicated for
44 about 15 min.

1
2
3
4
5
6
7
8
9
10
11
12
13
14
15
16
17
18
19
20
21
22
23
24
25
26
27
28
29
30
31
32
33
34
35
36
37
38
39
40
41
42
43
44
45
46
47
48
49
50
51
52
53
54
55
56
57
58
59
60
61
62
63
64
65

Loading of the Liquid Specimen TEM holder: A droplet (0.2 μl) of silica-ethanol suspension was placed on top of a Si microchip (Protochips Inc., NC, USA) supporting a Si_xN_y window of 50 nm thickness and dimensions of $20 \times 200 \mu\text{m}^2$. The microchip was plasma cleaned prior to loading to render the surface hydrophilic, and silica spheres were dispersed on the surface of the microchip. A dried microchip with silica was then positioned in the tip of a dedicated liquid-phase TEM holder (Protochips Inc., NC, USA), and a 0.5 μl droplet of either pure water or diluted (1:100) phosphate buffer saline solution (Roti[®]-Stock 10x, PBS) was placed on top. The liquid cell was then closed by placing the second microchip on top, with its membrane side facing downward. In this configuration, the microchip with silica nanoparticles was the top one once the holder was inserted in the electron microscope, such that the highest possible spatial resolution was obtained in the scanning TEM (STEM) mode for the downward traveling electron beam.^[4-8, 49, 50]

Electron Microscopy: Imaging was performed using an ARM200F (JEOL, Japan) microscope in either STEM or TEM mode at 200 keV electron beam energy. The following settings were used for STEM experiments: a probe current of 80 pA (6C electron beam probe size, 40 μm condenser lens aperture), and 8 cm camera length. STEM images of 512 x 512 pixels were collected with 20 μs pixel-dwell time. The electron dose for an image recorded at a typical magnification of 600,000 \times and a pixel size of 0.8 nm thus amounted to $1.6 \times 10^4 \text{ e}^-/\text{nm}^2$ (assuming that the electron dose was homogeneously distributed over a pixel area as a result of electron scattering by the silicon nitride membrane, nanoparticles, and the liquid). The electron dose rate was thus $3.0 \times 10^3 \text{ e}^-/\text{nm}^2/\text{s}$. During the experiments, water or PBS solutions were either kept static or flown at $4 \mu\text{l min}^{-1}$ through the cell. The TEM experiments were performed using 200 keV acceleration voltage, spot size 1, condenser lens aperture 1, and objective aperture 2. In case of TEM experiments, the sample was dispersed on the other

1 microchip so that it was at the bottom one once the holder is inserted in the microscope, thus
2 providing the best resolution for TEM.^[4-8, 51]
3
4

5 TEM images had a size of 1024x1024 pixels and the image acquisition time was 1 sec.
6
7

8 9 10 11 **Acknowledgments**

12 R. van den Berg and T. Parmentier are thanked for providing silica samples. J.Z. and K.J.
13
14 acknowledge funding from the NRSCC and European Research Council, an EU FP7 ERC
15
16 Advanced Grant no. 338846. NJ thanks Protochips Inc., NC, USA, for providing the liquid-
17
18 phase TEM system, and E. Arzt for his support through INM.
19
20
21
22

23 24 **Supporting Information**

25 Supporting Information is available from the Wiley Online Library or from the author. It
26
27 includes supporting Figures S1-S8 and Table S1, and Supporting Movie 1.
28
29
30
31

32 33 34 35 **References**

- 36
37
38
39 [1] J. Zecevic, K. P. de Jong, P. E. de Jongh, *Curr. Opin. Solid St. M.* **2013**, *17*, 115-125.
40
41 [2] A. K. Datye, *J. Catalysis* **2003**, *216*, 144-154.
42
43 [3] C. Kiely, *Nat. Mater.* **2010**, *9*, 296-7.
44
45 [4] N. de Jonge, F. M. Ross, *Nat. Nanotechnol.* **2011**, *6*, 695-704.
46
47 [5] J. M. Grogan, N. M. Schneider, F. M. Ross, H. H. Bau, *J. Indian Institute Sci.* **2012**,
48
49 *92*, 295-308.
50
51 [6] C. M. Wang, H. G. Liao, F. M. Ross, *Mrs Bull.* **2015**, *40*, 46-52.
52
53 [7] X. Y. Yu, B. W. Liu, L. Yang, *Microfluid. Nanofluid.* **2013**, *15*, 725-744.
54
55 [8] D. F. Parsons, *Science* **1974**, *186*, 407-414.
56
57
58
59
60
61
62
63
64
65

- 1
2
3
4
5
6
7
8
9
10
11
12
13
14
15
16
17
18
19
20
21
22
23
24
25
26
27
28
29
30
31
32
33
34
35
36
37
38
39
40
41
42
43
44
45
46
47
48
49
50
51
52
53
54
55
56
57
58
59
60
61
62
63
64
65
- [9] M. J. Williamson, R. M. Tromp, P. M. Vereecken, R. Hull, F. M. Ross, *Nat. Mater.* **2003**, *2*, 532-536.
- [10] K. L. Liu, C. C. Wu, Y. J. Huang, H. L. Peng, H. Y. Chang, P. Chang, L. Hsu, T. R. Yew, *Lab Chip* **2008**, *8*, 1915-21.
- [11] H. Zheng, S. A. Claridge, A. M. Minor, A. P. Alivisatos, U. Dahmen, *Nano Lett.* **2009**, *9*, 2460-5.
- [12] M. J. Dukes, B. W. Jacobs, D. G. Morgan, H. Hegde, D. F. Kelly, *Chem. Commun.* **2013**, *49*, 3007-9.
- [13] E. Jensen, C. Kobler, P. S. Jensen, K. Molhave, *Ultramicroscopy* **2013**, *129*, 63-9.
- [14] T. J. Woehl, K. L. Jungjohann, J. E. Evans, I. Arslan, W. D. Ristenpart, N. D. Browning, *Ultramicroscopy* **2013**, *127*, 53-63.
- [15] J. Y. Huang, L. Zhong, C. M. Wang, J. P. Sullivan, W. Xu, L. Q. Zhang, S. X. Mao, N. S. Hudak, X. H. Liu, A. Subramanian, H. Fan, L. Qi, A. Kushima, J. Li, *Science* **2010**, *330*, 1515-1520.
- [16] H. Zheng, R. K. Smith, Y. W. Jun, C. Kisielowski, U. Dahmen, A. P. Alivisatos, *Science* **2009**, *324*, 1309-12.
- [17] J. E. Evans, K. L. Jungjohann, N. D. Browning, I. Arslan, *Nano Lett.* **2011**, *11*, 2809-13.
- [18] D. Li, M. H. Nielsen, J. R. Lee, C. Frandsen, J. F. Banfield, J. J. De Yoreo, *Science* **2012**, *336*, 1014-8.
- [19] H. L. Xin, H. Zheng, *Nano Lett.* **2012**, *12*, 1470-1474.
- [20] T. J. Woehl, J. E. Evans, L. Arslan, W. D. Ristenpart, N. D. Browning, *Acs Nano* **2012**, *6*, 8599-8610.
- [21] K. L. Jungjohann, S. Bliznakov, P. W. Sutter, E. A. Stach, E. A. Sutter, *Nano Lett.* **2013**, *13*, 2964-2970.

- 1
2
3
4
5
6
7
8
9
10
11
12
13
14
15
16
17
18
19
20
21
22
23
24
25
26
27
28
29
30
31
32
33
34
35
36
37
38
39
40
41
42
43
44
45
46
47
48
49
50
51
52
53
54
55
56
57
58
59
60
61
62
63
64
65
- [22] P. J. Smeets, K. R. Cho, R. G. Kempen, N. A. Sommerdijk, J. J. De Yoreo, *Nat. Mater.* **2015**, *14*, 394-9.
- [23] T. Kraus, N. de Jonge, *Langmuir* **2013**, *29*, 8427-32.
- [24] E. A. Ring, N. de Jonge, *Micron* **2012**, *43*, 1078-1084.
- [25] X. Chen, J. Wen, *Nanosci. Res. Lett.* **2012**, *7*, 598.
- [26] E. R. White, M. Mecklenburg, B. Shevitski, S. B. Singer, B. C. Regan, *Langmuir* **2012**, *28*, 3695-3698.
- [27] A. Radisic, P. M. Vereecken, J. B. Hannon, P. C. Searson, F. M. Ross, *Nano Lett.* **2006**, *6*, 238-242.
- [28] M. Gu, L. R. Parent, B. L. Mehdi, R. R. Unocic, M. T. McDowell, R. L. Sacci, W. Xu, J. G. Connell, P. H. Xu, P. Abellan, X. L. Chen, Y. H. Zhang, D. E. Perea, J. E. Evans, L. J. Lauhon, J. G. Zhang, J. Liu, N. D. Browning, Y. Cui, I. Arslan, C. M. Wang, *Nano Lett.* **2013**, *13*, 6106-6112.
- [29] R. L. Sacci, N. J. Dudney, K. L. More, L. R. Parent, I. Arslan, N. D. Browning, R. R. Unocic, *Chem. Commun.* **2014**, *50*, 2104-2107.
- [30] D. Alloyeau, W. Dachraoui, Y. Javed, H. Belkahla, G. Wang, H. Lecoq, S. Ammar, O. Ersen, A. Wisnet, F. Gazeau, C. Ricolleau, *Nano Lett.* **2015**, *15*, 2574-81.
- [31] D. B. Peckys, N. de Jonge, *Microsc. Microanal.* **2014**, *20*, 346-365.
- [32] H. Nishiyama, M. Suga, T. Ogura, Y. Maruyama, M. Koizumi, K. Mio, S. Kitamura, C. Sato, *J. Struct. Biol.* **2010**, *169*, 438-49.
- [33] B. L. Gilmore, S. P. Showalter, M. J. Dukes, J. R. Tanner, A. C. Demmert, S. M. McDonald, D. F. Kelly, *Lab chip* **2013**, *13*, 216-9.
- [34] N. M. Schneider, M. M. Norton, B. J. Mendel, J. M. Grogan, F. M. Ross, H. H. Bau, *J. Phys. Chem. C* **2014**, *118*, 22373-22382.
- [35] J. M. Grogan, N. M. Schneider, F. M. Ross, H. H. Bau, *Nano Lett.* **2014**, *14*, 359-64.

- 1
2
3
4
5
6
7
8
9
10
11
12
13
14
15
16
17
18
19
20
21
22
23
24
25
26
27
28
29
30
31
32
33
34
35
36
37
38
39
40
41
42
43
44
45
46
47
48
49
50
51
52
53
54
55
56
57
58
59
60
61
62
63
64
65
- [36] J. M. Yuk, J. Park, P. Ercius, K. Kim, D. J. Hellebusch, M. F. Crommie, J. Y. Lee, A. Zettl, A. P. Alivisatos, *Science* **2012**, *336*, 61-4.
- [37] K. L. Jungjohann, J. E. Evans, J. A. Aguiar, I. Arslan, N. D. Browning, *Microsc. Microanal.* **2012**, *18*, 621-7.
- [38] M. W. van de Put, C. C. Carcouet, P. H. Bomans, H. Friedrich, N. de Jonge, N. A. Sommerdijk, *Small* **2015**, *11*, 585-90.
- [39] D. S. Li, M. H. Nielsen, J. J. De Yoreo, *Method. Enzymol.* **2013**, *532*, 147-164.
- [40] M. Liong, J. Lu, M. Kovochich, T. Xia, S. G. Ruehm, A. E. Nel, F. Tamanoi, J. I. Zink, *ACS Nano* **2008**, *2*, 889-896.
- [41] S. H. Joo, J. Y. Park, C. K. Tsung, Y. Yamada, P. D. Yang, G. A. Somorjai, *Nat. Mater.* **2009**, *8*, 126-131.
- [42] G. Prieto, J. Zecevic, H. Friedrich, K. P. de Jong, P. E. de Jongh, *Nat. Mater.* **2013**, *12*, 34-39.
- [43] R. van den Berg, T. E. Parmentier, C. F. Elkjaer, C. J. Gommers, J. Sehested, S. Helveg, P. E. de Jongh, K. P. de Jong, *ACS Catal.* **2015**, *5*, 4439-4448.
- [44] A. Verch, M. Pfaff, N. De Jonge, *Langmuir* **2015**, *31*, 6956-6964.
- [45] J. Hermannsdoerfer, N. de Jonge, A. Verch, *Chem. Comm.* **2015**, *51*, 16393-16396.
- [46] S. H. A. Chan, *Geotherm.* **1989**, *18*, 49-56.
- [47] T. van Dillen, A. Polman, C. M. van Kats, A. van Blaaderen, *Appl. Phys. Lett.* **2003**, *83*, 4315-4317.
- [48] W. Stoeber, A. Fink, E. Bohn, *J. Colloid Interface Sci.* **1968**, *26*, 62-69.
- [49] N. de Jonge, N. Poirier-Demers, H. Demers, D. B. Peckys, D. Drouin, *Ultramicroscopy* **2010**, *110*, 1114-1119.
- [50] T. Schuh, N. de Jonge, *C. R. Phys.* **2014**, *15*, 214-223.
- [51] K. L. Klein, I. M. Anderson, N. de Jonge, *J. Microscopy* **2011**, *242*, 117-123.

Online Supporting Material

Anisotropic Shape Changes of Silica Nanoparticles Induced in Liquid with Scanning Transmission Electron Microscopy

Jovana Zečević, Justus Hermannsdörfer, Tobias Schuh, Krijn P. de Jong, Niels de Jonge

1. Liquid Flow

A series of experiments was conducted under liquid flow conditions in which the microfluidic chamber in the liquid flow sample holder was continuously flushed with water, see Figure S1. Similar elongation and shrinking was observed as for the static case in which liquid was not flown through the system shown in Figure 1 of the main text.

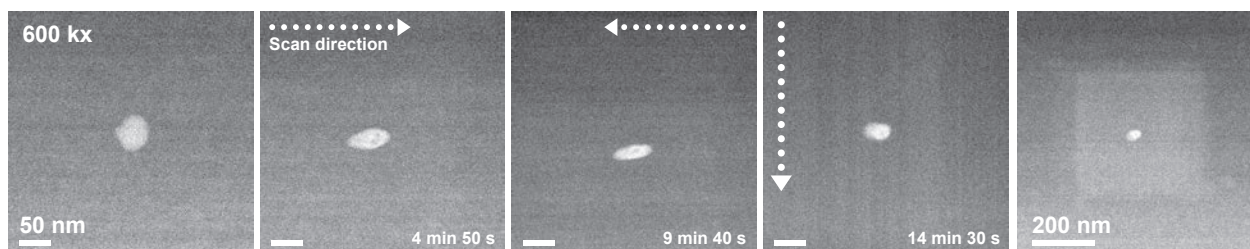


Figure S1. Liquid-phase scanning transmission electron microscopy (STEM) time-lapse experiment of individual silica nanoparticles under liquid flow conditions. Row of five images of a nanoparticle in pure water showing elongation, at a magnification $M = 600,000\times$. The scan direction was changed between the images. Also deposition of carbon (see below) on the supporting silicon nitride membrane is visible from the rectangular shape in the panel at the right lower corner recorded at a lower magnification.

2. Measurement of Particle Sizes

The sizes of the silica nanoparticles shown in Figure 1 of the main text were measured in both horizontal- and vertical direction. A transition from a dark to a bright grey value in the image was taken as measure of the edge of a nanoparticle as shown in Figure S2. Horizontal and vertical widths were measured from the first frame before particles were exposed to prolonged scanning, and after each cycle of 7 cycles of scanning as indicated in the Table S1. The scan direction was alternated between horizontal and vertical as indicated in Figure 1 of the manuscript.

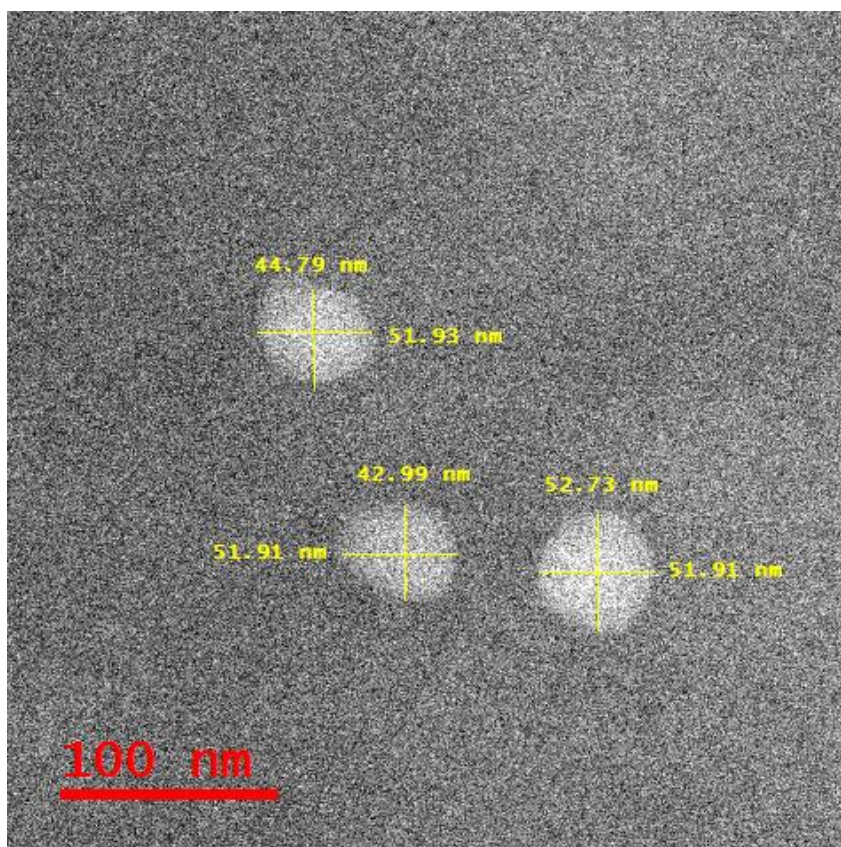


Figure S2. Liquid-phase scanning transmission electron microscopy (STEM) image with included measurements of nanoparticle sizes in horizontal- and vertical direction.

Table S1. Measurement of nanoparticle widths in horizontal and vertical directions at the beginning and after each scan cycle. Scan direction was alternated between horizontal (cycles 1, 3, 5 and 5) and vertical (cycles 2,4 and 6) direction.

Particle #	Direction	Start	Cycl 1	Cycl 2	Cycl 3	Cycl 4	Cycl 5	Cycl 6	Cycl 7
1	Vertical	44.8	31.6	38.1	27.1	36.5	21.8	30	20.3
	Horizontal	51.9	57.2	40.6	45.2	26.8	33.1	19.5	21.1
2	Vertical	43	31.6	36.5	28.6	31.6	22.6	25.2	21.8
	Horizontal	51.9	55.7	38.1	39.9	26.8	31.6	19.5	21.8
3	Vertical	52.7	33.9	39.7	27.1	35.7	20.3	30.8	27.1
	Horizontal	51.9	56.4	38.1	45.9	30	37.6	22.7	22.6

3. Measurement of the Particle Thickness

A further set of experiments was conducted at 600k magnification in which the elongation of the silica nanoparticles was observed, see Figure S3. The particles were enlarging in the direction of the scanning beam. The dose rate was $30 \text{ e}^-/\text{Å}^2/\text{s}$. Line profiles of intensity in the image along the particles were analyzed to study the dose dependent effect. The signal intensity in dark field STEM is a function of the charge density in the material and thus increases with increasing amount of material in the beam path. The line profiles verify that the nanoparticle elongated. Since the signal intensity in the middle of the nanoparticle remained constant within the statistical fluctuation, it can be concluded that the nanoparticle did not significantly change its shape in the direction perpendicular to the imaging plane.

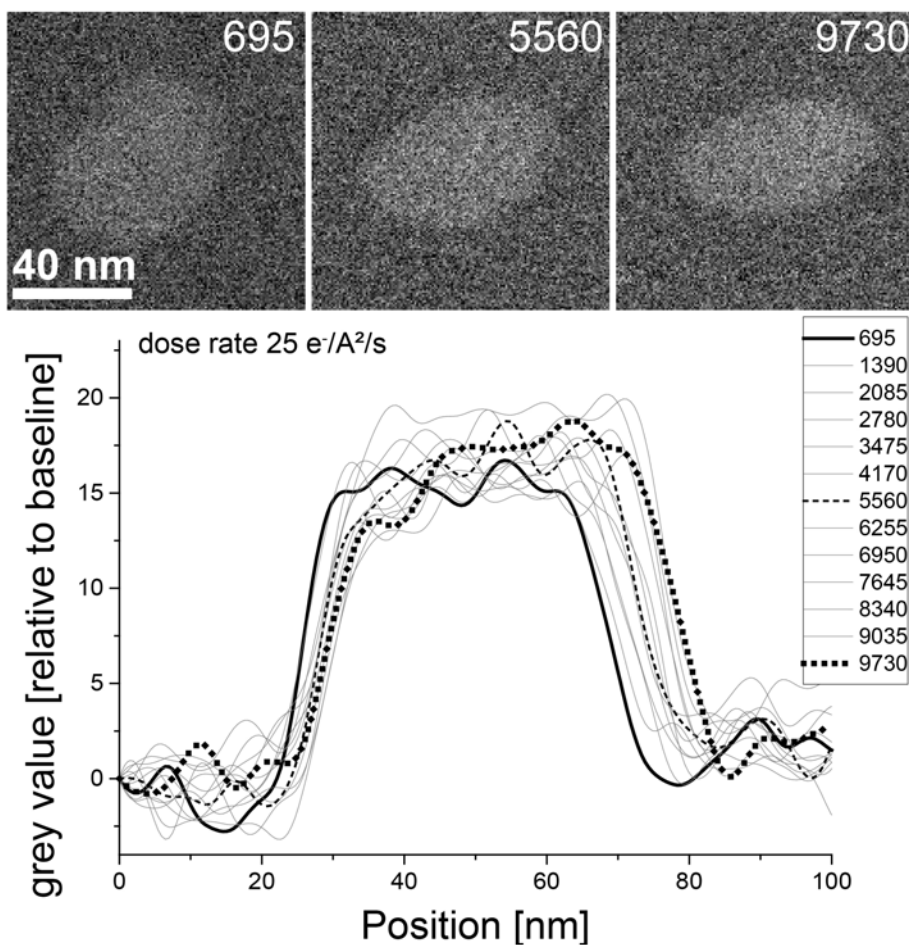


Figure S3. Three liquid-phase STEM images with included measurements of the signal intensity over the nanoparticle in horizontal direction for different electron doses. The electron dose in e^-/nm^2 is given for the three images and for all line scans.

In order to further analyze the three-dimensional shape of the silica nanoparticles, we examined a dried sample in vacuum of three nanoparticles that had been exposed to the electron beam in liquid. The microchip with silica nanoparticles was first irradiated with the electron beam in liquid, then the microchip with the specimen was removed from the liquid holder, dried and studied in vacuum with transmission electron microscopy (TEM). Images were acquired under different tilt angles of the sample stage (first row of Figure S4). The

sample was exposed in liquid for 6 min to a dose rate of $30 \text{ e}^-/\text{Å}^2/\text{s}$. The experiment was repeated for a second sample (represented in the second row of Figure S4). This sample was exposed in liquid for 21 min to a dose rate of $30 \text{ e}^-/\text{Å}^2/\text{s}$. Since the particle sizes at titles projection angles did not appear to be enlarged, the occurrence of vertical elongation during electron beam irradiation can be ruled out.

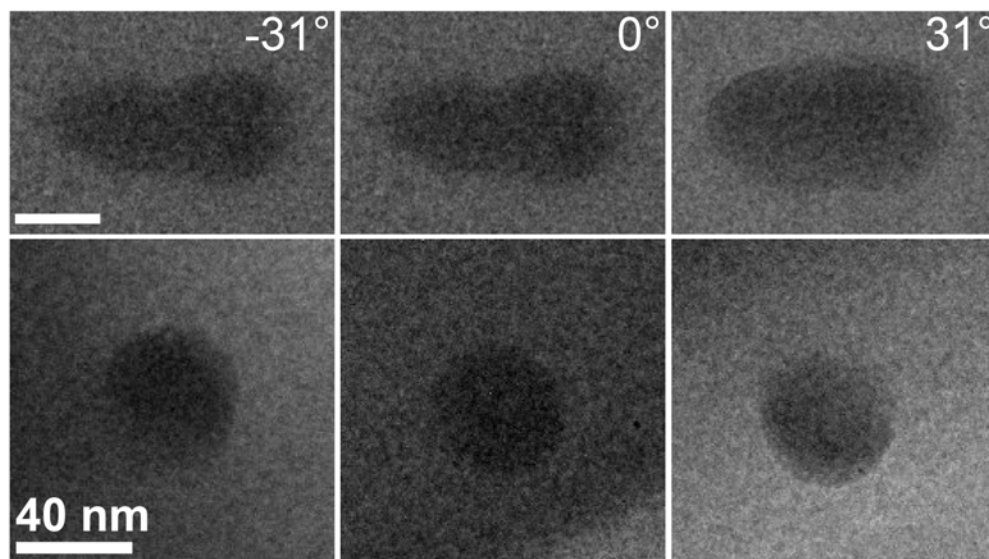


Figure S4. Transmission electron microscopy (TEM) images at different tilt angles of the sample stage of nanoparticles in vacuum exposed to the electron in liquid prior to the TEM experiment.

4. Elemental Analysis of Silica Nanoparticles

Another sample with silica nanoparticles was first irradiated with the electron beam in liquid, then the microchip with the specimen was removed from the liquid holder, dried and studied in vacuum with STEM and energy dispersive X-ray (EDX) analysis (Figure S5). This sample was exposed in liquid for 4 min to a dose rate of $30 \text{ e}^-/\text{Å}^2/\text{s}$. The square bright area appearing after repeated image acquisition at the same position appears to have been carbon. The silicon signal is visible over the entire image as a result of the silicon nitride window and the strongest signal is visible at the location of the nanoparticle. The nanoparticle also contains

oxygen. Importantly, the nanoparticle did not contain carbon and appears homogeneous in composition.

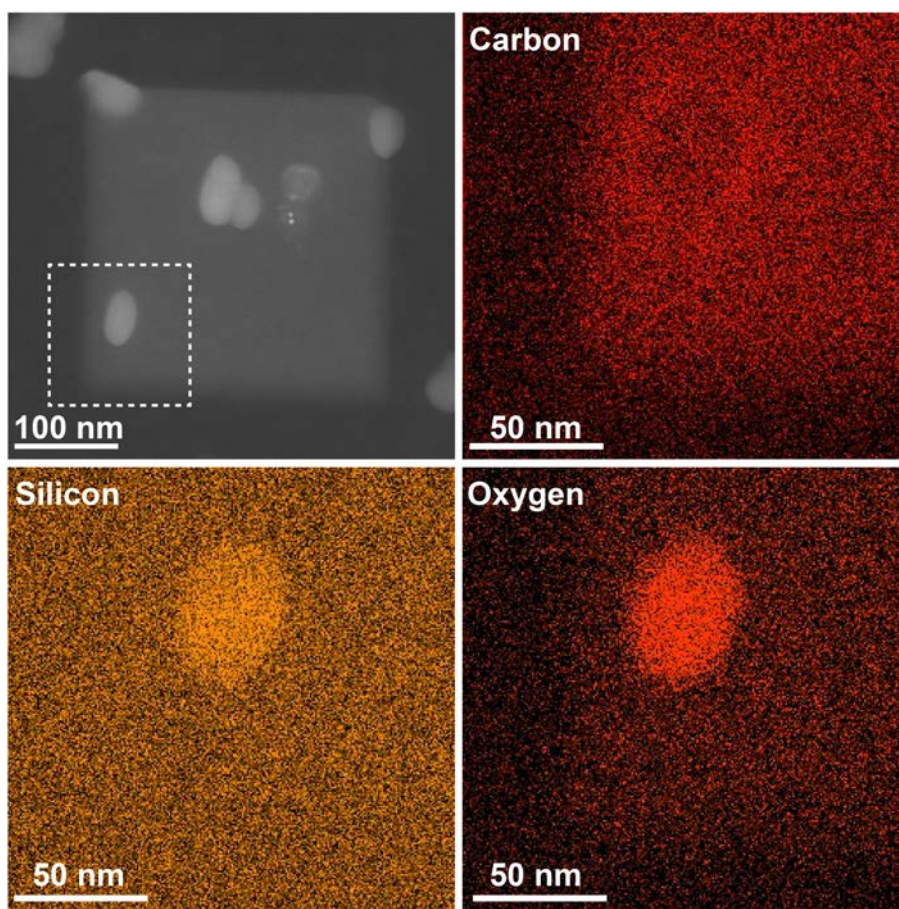


Figure S5. Vacuum STEM of silica nanoparticles exposed to a dose rate of $25 \text{ e}/\text{A}^2/\text{s}$ in liquid. (left top) Silica nanoparticles with a homogeneous structure imaged with STEM of a dried sample in vacuum. (tight top) Energy dispersive X-ray (EDX) analysis of the carbon spectrum. (bottom) EDX of the silicon (left) and oxygen (right) spectrum.

5. Examination of the Nanoparticle Stability in Vacuum

To test for possible structural changes without the presence of liquid, a further series of experiments was conducted in which a sample with fresh nanoparticles was placed on a silicon nitride membrane, dried and irradiated during STEM in vacuum (Figure S6). Some structural rearrangement took place for very high doses but the severe shrinking of one side

and the elongation of the other side was not observed. The alteration of the shape of the SiO₂ nanoparticles in vacuum is due to deposition of electron beam energy and thus a heating of the nanoparticle. The surface of the SiO₂ nanoparticle cannot be cooled as in the case of surrounding water.

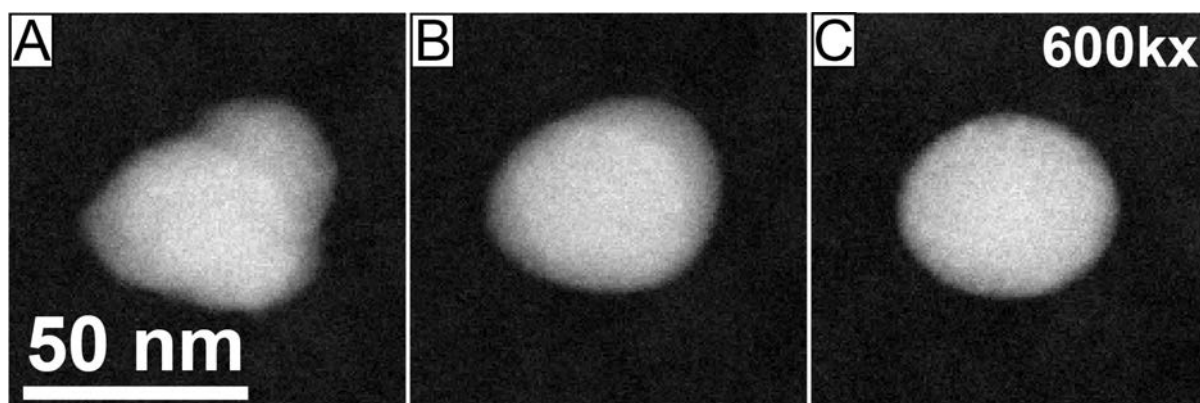


Figure S6. STEM experiment at very high electron doses in vacuum of nanoparticle that was not exposed to the electron beam in liquid. (a) First image recorded with a dose of $1 \times 10^4 \text{ e}^-/\text{nm}^2$. (b) Image recorded after 25 min of continuous imaging with a total electron dose of $3.7 \times 10^6 \text{ e}^-/\text{nm}^2$ (25 min). (c) Total dose of $8.2 \times 10^7 \text{ e}^-/\text{nm}^2$ (55 min).

6. Nano-Doughnuts

The vertical shape of the nanoparticles with holes in the middle (nano-doughnuts) were studied at a magnification of 1.2M in which the dose rate was increased to $100 \text{ e}^-/\text{Å}^2/\text{s}$, see Figure S7. Line profiles of intensity along the changing particles were analyzed. Here, the formation of wholes becomes visible after an applied dose of $1600 \text{ e}^-/\text{Å}^2$, as follows from the reduction of the signal intensity in the middle.

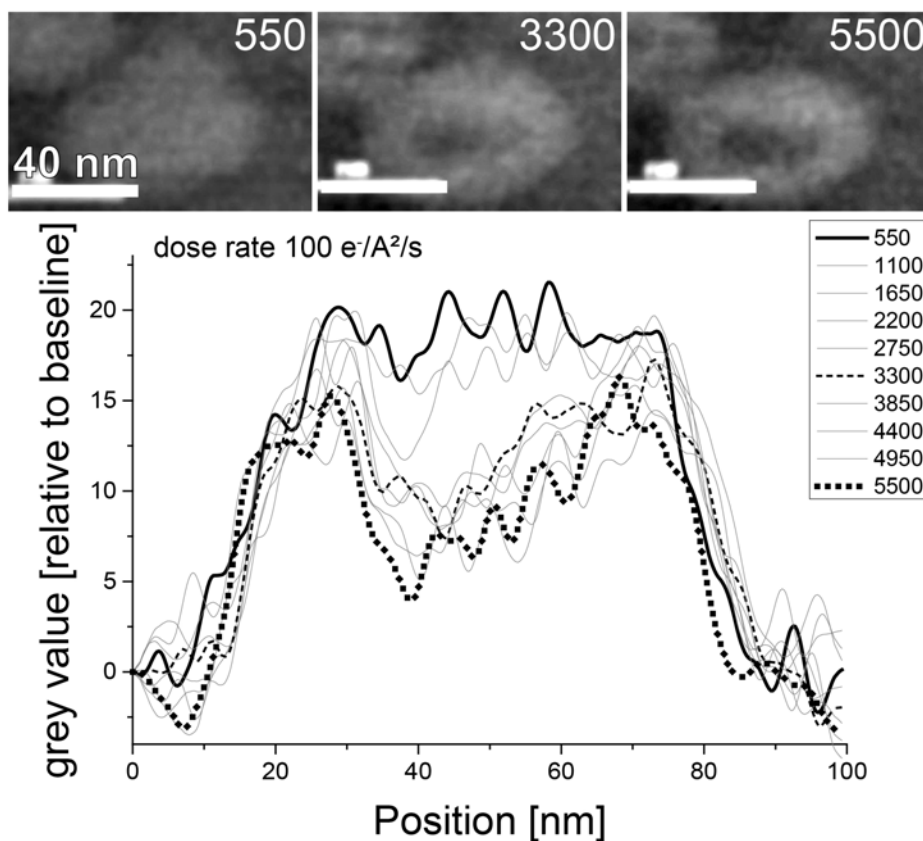


Figure S7. Liquid-phase STEM recorded at a dose rate of $100 \text{ e}^-/\text{nm}^2/\text{s}$ including measurements of the signal intensity over the nanoparticle in horizontal direction for different electron doses in e^-/nm^2 .

6. Contamination

While a nano-doughnut was created at high dose, a square in the image appeared. This sample was removed from the liquid holder, dried, and studied with vacuum STEM. Figure S8 top row shows that also the dried sample showed an absence of material from the middle of the nanoparticles (lower STEM signal). The nanoparticles contain indeed silicon as was verified using EDX analysis. Also here, the squared area appeared to be carbon contamination. From tilting experiments it followed that the carbon contamination was on the other side of the silicon nitride membrane as the nanoparticles (data not shown)

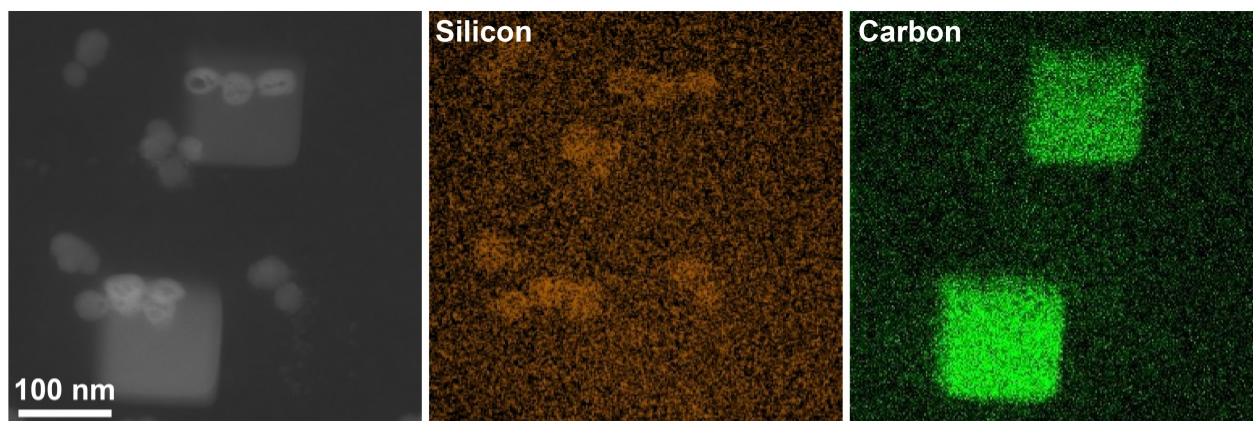


Figure S8. Vacuum STEM of silica nanoparticles exposed to a dose rate of $100 \text{ e}^-/\text{Å}^2/\text{s}$ in liquid. (left) Silica nanoparticles with a hole in the middle (nano-doughnuts) imaged with STEM of a dried sample in vacuum. (middle) Energy dispersive X-ray (EDX) analysis of the silicon spectrum. (right) EDX of the carbon spectrum.